Spring 2021

Liquid Rocket Engine and Test System

Ronnie Wallingford
The University of Akron, rew63@uakron.edu

Grace Ann Phillips
The University of Akron, gap43@uakron.edu

Blake Bowser
The University of Akron, bab195@uakron.edu

Jack Dalton
The University of Akron, jwd45@uakron.edu

LIQUID ROCKET ENGINE AND TEST SYSTEM

Final Report for 4600:402-461/4600:402-497 Senior/Honors Design

By:
Blake Bowser
Jack Dalton
Grace Phillips
Ronnie Wallingford

Project Sponsor: Dr. Manigandan Kannan

Honors Department Advisor: Dr. Scott Sawyer

Honors Reader 1: Dr. Francis Loth

Honors Reader 2: Charles Campbell

3 May 2021
Mechanical Engineering Senior Project No. 38

ABSTRACT

The goal of this project is to design the University of Akron's first design team built liquid propulsion rocket engine and testing system. Liquid propulsion rocket engines are widely used on space launch vehicles in comparison to solid phase propulsion engines and other engine types such as hypergolic engines and liquid hybrid engines, however in the collegiate rocketry environment they are less frequently used due to their complexity and high cost. The creation of this engine and testing system will create new opportunities for the Akronauts Rocket Design Team moving forward, allowing the team to enter more prestigious competitions, and will also enable students to better pursue opportunities in the space and defense industry by exposing them to more relevant industry experiences.

The liquid rocket engine designed by the team will utilize ethanol and liquid nitrous oxide to generate approximately 500 lbf of thrust. An accompanying test system was designed for this motor with modularity and safety in mind. These design foci will enable the team to safely test motors of various thrust capacities without needing to make major modifications to the system.

To verify the safety of the rocket engine and testing system, the team did hand calculations and computer analysis of critical components and their designs. To further verify the safety and functionality of the systems, physical testing of individual components and assembled subsystems will be completed once components are acquired.

TABLE OF CONTENTS

TABLE OF FIGURES

TABLE OF EQUATIONS

TABLE OF TABLES

1. INTRODUCTION

This project aims to design a liquid rocket engine and testing system in order to help expand the design team's knowledge of liquid engine propulsion. The design is motivated by the desire to gain industry relevant experience utilizing engineering skills learned from fluid mechanics, mechanical metallurgy, heat transfer, concepts of design, and chemistry. The knowledge and design of the liquid engine and test stand would help make the Akronauts Rocket Design Team stand out at competition, as very few collegiate design teams have successfully developed liquid rocket engines. The design team has previously designed and manufactured solid rocket engines, however the development of a liquid engine would help the team gain more industry recognition and experience for industry applications, as well as be a powerful recruitment tool for the design team and the University. The liquid engine would also allow the team to use propellants with higher efficiencies. The use of a testing system would help the team safely test the propellant chemicals. The testing system design would ideally be a mobile system located on a trailer bed, and it would utilize an 80/20 adjustable rail with fire walls between the engine, tanks, and controls.

1.1. PROJECT OBJECTIVES

The goal of this project is to design a liquid rocket engine and an accompanying testing system. To meet this goal, the team has outlined the following key objectives: system design, project safety, and system fabrication and verification.

The system design encompasses both conceptual design of the engine and physical design of the engine and test stand. These two design subsets are important to distinguish, as the conceptual design is what defines the physical dimensions of the motor and gives critical values for the safe design of system components. Once these dimensions and values are determined, the components can be designed with manufacturability, modularity, and strength in mind. For this objective, the goal was to design an engine that could generate approximately 500 lbf of thrust and would safely operate with an oxidizer vapor pressure of 750 psi and a test stand that could withstand and record the motor thrust.

Project safety is very important to the success of this project. This objective was broken down into the testing and design verification of the systems and University Safety approval. Design verification was done using hand calculations and computer simulations to ensure that the factors of safety in the system components were appropriate. Testing the components to verify they operate as intended will ensure that the system also operates safety. University Safety approval was important to get to progress with project construction and testing and to get outside verification on the safety of the project. Unfortunately, obtaining approval to construct the engine and test stand through the university's safety department proved to be a long process.

Ideally this project would result in the fabrication of the rocket engine and test system and subsequent testing to verify their performance, however the global coronavirus pandemic has caused considerable financial strain to the University and the Akronauts Rocket Design Team, so funding for this project is very limited. Additionally, due to the delay in getting university safety approval, the acquisition and assembly of components was delayed and will be completed by the Akronauts once the project is passed on to the design team.

2. DESIGN

For this project, the design process was broken up into two stages: the conceptual design of the engine and the physical design of key components and assemblies. The conceptual design was completed first to determine key performance information from the system. Once this design stage was complete, values and geometries from the conceptual design were used in the design process of the physical components to ensure that the system could be manufactured and would operate safely.

2.1. CONCEPTUAL DESIGN

There were two key components to the conceptual design of the engine: the propellant selection and motor geometry. Before a conceptual design for the motor geometry can be created the propellants used in the system needed to be determined. Once the propellants were determined, their known properties and combustion characteristics were used to generate a motor geometry that meet the pressure and thrust goals of the system.

2.1.1. PROPELLENT SELECTION

The liquid bi-propellant rocket engine will feature an oxidizer and fuel that will be combined at equal pressure inside the combustion chamber prior to ignition. The team chose to use Liquid Nitrous Oxide as the oxidizer and Ethanol as the fuel for the engine. These propellants were selected as they are the safest to use and easiest to acquire of the propellants considered. A comparison of the considered propellants can be seen below in **Figure 1**. The team's decision to use these propellants was approved by the University of Akron's safety department.

Fuels

- Ethanol → Our current choice
    - Non-toxic and environmentally friendly
    - Long history as rocket propellant
    - Used in performance cars
    - Easy to acquire
- Kerosene
    - More efficient than ethanol
    - Less seal-friendly
- Liquid Methane
    - Cryogenic
    - High efficiency
- Liquid Hydrogen
    - Cryogenic
    - Most efficient fuel
    - Leaks through most seals
    - Extremely high vapor pressure

Oxidizer

- Liquid Nitrous Oxide → Our current choice
    - Non-cryogenic
    - Readily available commercial handling equipment
    - Used in TRA approved hybrid propulsion systems and performance vehicles
- Liquid Oxygen
    - Cryogenic
    - Very efficient
- High Test Peroxide
    - Not allowed at competition
    - Requires catalyst bed
    - Requires special protective gear
- Liquid Fluorine
    - Best oxidizer
    - Extremely toxic

Figure 1 – Propellant Choices

To operate the engine, pre-pressurized nitrous oxide vapor will be used to drive a piston that pressurizes the ethanol. Just before the injection plate, independently controlled regulator valves will be used to equalize the pressures.[1] A diagram of this system can be seen below in **Figure 2**.

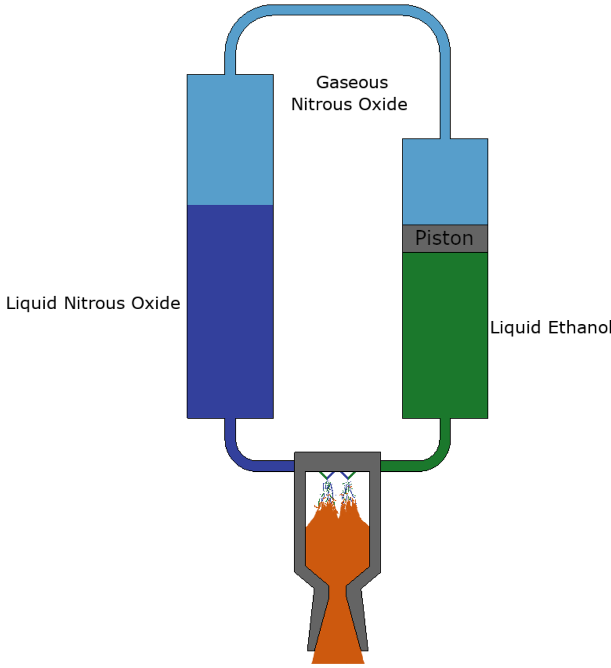

Figure 2 – Basic Depiction of a VAPAK Feed System Setup (Drawn by Charles Campbell)

2.1.2. CONCEPTUAL MOTOR DESIGN

ProPep3 is a propellant analysis program typically used for solid phase motors. This program has assisted UA's rocket design team in created SRAD (student researched and designed) solid fuel motors for the past few years. It gives basic data from a motor's chemical concentration and outputs items such as specific impulse, combustion chamber temperature, and so on. Assuming a combustion chamber pressure of 400psi, the system will have an approximate combustion chamber temperature of 3000K and a specific impulse of 200s based on a 4:1 oxidizer-fuel ratio for 298 K Nitrous-Oxide and 95% Ethanol.[2,3,4] This information provides clarity on the need for thermal protection when selecting what type of material will be used for the main components of the engine. As explained by the team in the proposal, the team will be using mainly aluminum engine parts for safety reasons, as aluminum is widely recognized as a non-frangible material, unlike many steels. The program outputs can be seen below, in **Figure 3**.

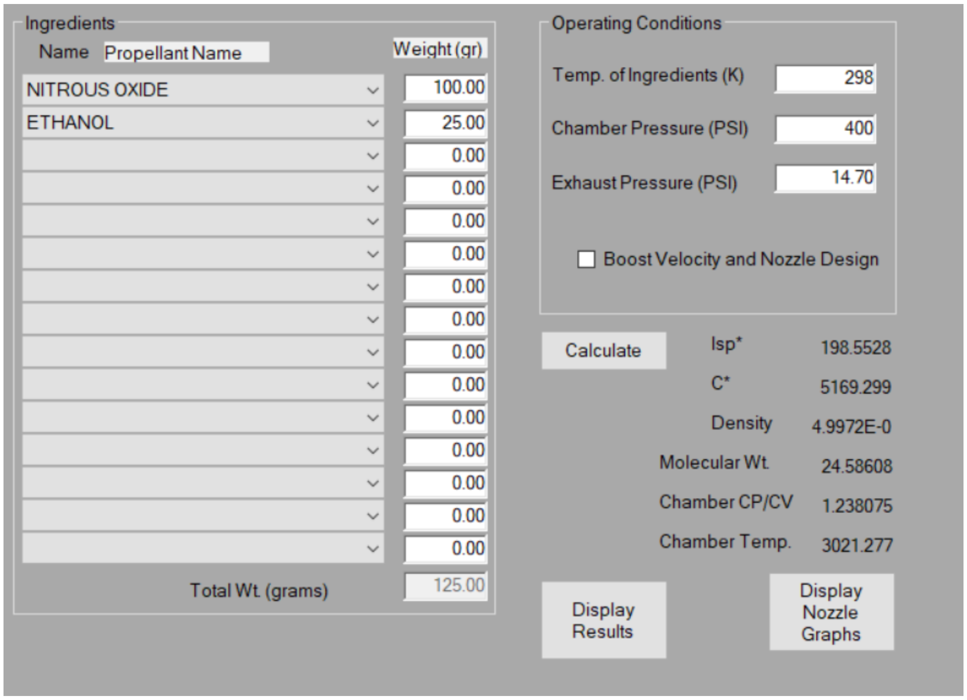

Figure 3 – ProPep3 Output

With this in mind, one can use Fourier's Law for radial heat travel in cylinders (**Equation 1**) to examine the heat conduction through the aluminum combustion chamber and note that for a relative burn time of 5-10s, there will be enough heat conduction to make aluminum fail as a pressure holding device. This means that a thermal protection system will need to be in place to keep the engine from failing due to thermal degradation in the material. A cheap and simple way to do this is by using a phenolic combustion chamber liner, which is often used for solid rocket boosters and amateur rocketry engines. Phenolic liners are well insulating tubes of a phenolic cardboard mixture that is one time use but will protect the engine long enough for a stable and successful burn. The team will alternatively utilize a mix of epoxy and phenolic microbeads for a castable version of this component.

$$Q = \frac{2\pi k L (T_i - T_e)}{\ln\left(\frac{r_e}{r_i}\right)}$$

Equation 1 – Fourier's Law for Radial Heat Travel in Cylinders

The throat of the engine will also have to be thermally protected since it will be experiencing a large amount of heat. This can be done by using a graphite insert for the throat of the converging diverging system. Graphite can handle heat and pressure much better in comparison to aluminum and will withstand the heat with the approximate burn times mentioned above.

RPA (Rocket Propulsion Analysis) is a liquid engine program that takes a multi-variable, multi-input approach at dimensioning an engine based on general constraints, fuel and oxidizer, mixture ratio, atmospheric conditions, and many others.[5] The program outputs expected engine thrust when optimized for the input conditions as well as vacuum conditions. These results can be hand calculated using the equations in **APPENDIX B: EQUATIONS FROM CAMPBELL ET AL[1]** and following the process outlined in the "Design and Testing of a Low-Cost Bipropellant Liquid Rocket Engine."[1] Our team used this program as shown below in **Figure 4**.

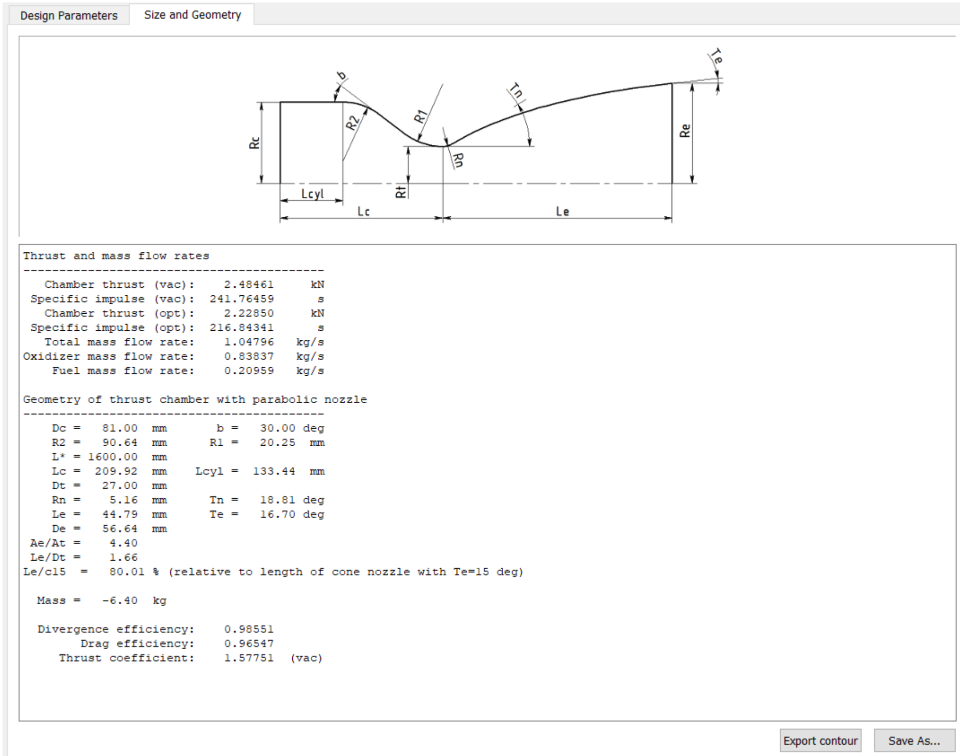

Figure 4 – RPA Output

Thus, the team’s expected engine parameters shown will output an optimized thrust (at sea level) of 2.23kN (~510lbf) and a vacuum thrust of 2.48kN (~557lbf) when in space. This is advantageous as thrust will not be lost but gained for the engine when propelling through the atmosphere. At the team’s scale, this will be useful. However, in industry, staged liquid rocket booster engines would need to be optimized for the various layers of the atmosphere as to lower cost (fuel waste) and an increase in general efficiency. Flow exit expansion is shown in **Figure 5** provided by Stephen Heister et al.[6]

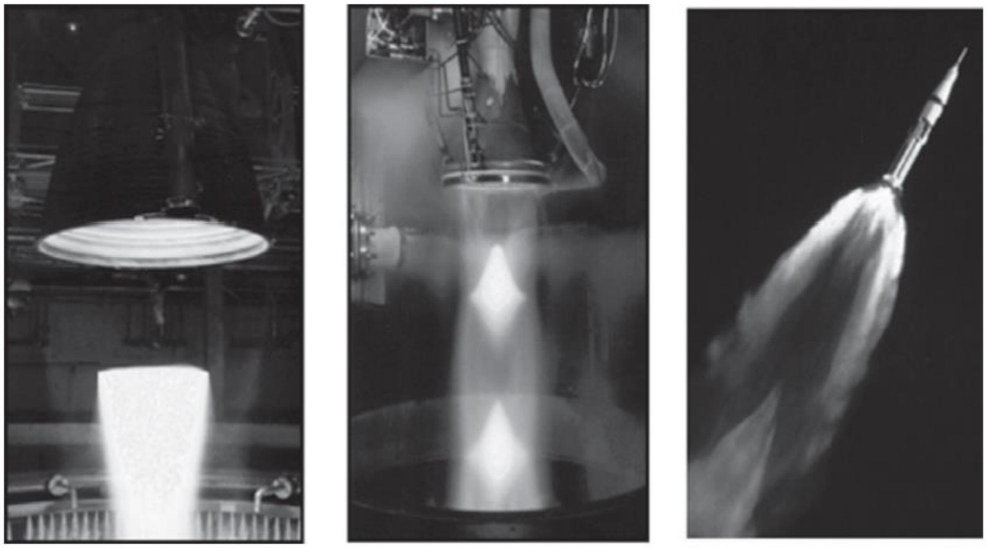

Figure 5 – Over-expanded, perfectly expanded (most efficient), and under-expanded flow examples, courtesy of Heister et al[6]

The other important quantity in regards to engine characterization is the specific impulse, which measures an engine's efficiency with respect to thrust and fuel weight flow rate. This can be calculated using **Equation 2**.

$$I_{sp} = \frac{F}{\dot{m}g}$$

Equation 2 – Specific Impulse

The team's engine shows a specific impulse of approximately ~200s in ProPep3, and an impulse of ~240s using RPA. RPA shows a more accurate value, since it involves more information regarding the engine, aside from just propellant choices.

RPA also outputs fuel consumption based on the engine performance. It is shown that the engine will require approximately 1.04kg/s of total mass flow, 0.84kg/s of oxidizer, and 0.21kg/s of fuel. Assuming a 6 second burn time, the team can supply the engine with ~5.24kg (11.5lb) of oxidizer, and ~1.31kg (2.88lb) of fuel. Therefore, the team must account volumetrically for each of these tank sizes on the testing system.

Using the values from RPA, the specific impulse can be hand-calculated through the following equations, found in Stephen Heister et al.[6] Throat pressure can be solved for using chamber pressure and the specific heat ratio, as seen below in **Equation 3**.

$$\frac{p_c}{p_t} = \left[\frac{\gamma + 1}{2}\right]^{\frac{\gamma}{\gamma - 1}}$$

Equation 3 – Used to Find Throat Pressure

Assuming choked flow, **Equation 4** can be used to find the throat area.

$$\dot{m} = \frac{\gamma p_t A_t}{a_t}$$
Equation 4 – Used to Find Throat Area

Using a traditional hand calculation approach, the Mach flow at the exit is found from **Equation 5**.

$$M_e = \sqrt{\left(\frac{2}{\gamma - 1}\right)\left[\left(\frac{p_c}{p_a}\right)^{\frac{\gamma-1}{\gamma}} - 1\right]}$$
Equation 5 – Mach Flow at the Exit

Using the previously calculated values, the exit area can be calculated using **Equation 6**.

$$A_e = \left(\frac{A_t}{M_e}\right)\left[\frac{1 + \left(\frac{\gamma - 1}{2}\right)M_e^2}{\left(\frac{\gamma + 1}{2}\right)}\right]^{\frac{\gamma+1}{2(\gamma-1)}}$$
Equation 6 – Exit Area

Using the previous two solved values, **Equation 7** can be used to calculate thrust with the inclusion of p_a and p_e.

$$F = \dot{m}V_e + (p_e - p_a)A_e$$
Equation 7 – Thrust

The general mass flow equation is shown in **Equation 8**, below.

$$\dot{m} = \rho V A$$
Equation 8 – Mass Flow

Mass flow rates of the oxidizer and fuel can be separated in the following equations:

$$\dot{m_f} = \frac{\dot{m}}{1 + r}$$
Equation 9 – Fuel Mass Flow Rate

$$\dot{m_{ox}} = \frac{r\dot{m}}{1 + r}$$
Equation 10 – Oxidizer Mass Flow Rate

A comprehensive list of the variables used in this document can be found in **APPENDIX A: EQUATION VARIABLES**.

2.2. PHYSICAL DESIGN

Using the values and geometries derived from the conceptual design section, physical designs for the motor, feed systems, test stand, and oxidizer and fuel tanks were created. The design of these components focused on the manufacturability, modularity, and safety of the systems.

When accounting for the repeatability of tests, the system was designed to easily be able to refill the test engine's fuel and oxidizer tanks. A plan was set in place to use a combination of a check valve, hand valve, and solenoid valve to actuate the re-filling of the oxidizer portion of the engine. The fuel tank will have to be removed from the test stand by hand and refilled due to the piston pressurization application being used to obtain equal pressure output of the fuel and oxidizer. The convenience of also having the engine portion of the design modular, will also assist the team in replacing the single use phenolic liner for the combustion chamber. The downside of this is that the engine will not be able to be fired back-to-back without direct human intervention. This does conveniently allow for direct post-burn operational assessment for the system after each test, which is beneficial for characterizing the possible faults of the system from single test runs.

2.2.1. MOTOR

The motor is the most essential component of the rocket, and the rest of the components are built around the motor to achieve the best performance. The motor is basically a pressure vessel that is built to contain and direct the combustive energy. The designed motor can be seen below in **Figure 6**. The aft of the motor case will contain the nozzle, and the motor casing will be insulated with a thin layer of phenolic liner. The oxidizer (nitrous oxide) and fuel (ethanol) will be pressurized before reaching the injection plate.[7] From there the mixture will enter the combustion chamber at equal pressures. The nozzle is responsible for accelerating the combusted gases through a converging-diverging profile at supersonic speeds. Due to the high levels of heat the nozzle experiences, the nozzle will be made of graphite. The nozzle must be machined with a high degree of accuracy to achieve the smooth and precise geometry needed for stable flight. Efficiency of the thrust is determined by the shape of the nozzle. Longer nozzles with shallower angles through the converging duct yield the best efficiency, however, they will also increase viscous drag and weight. Due to this tradeoff, simulations were performed to maximize the power output.[1]

Figure 6 – Isometric view of Motor

The motor design has been finalized, and the manufacturing process has begun. The motor is designed to have a flanged connection between the injector plate and chamber, and an ID retention snap ring for the nozzle and aluminum retaining core. The nozzle was designed to be manufactured from graphite since it is a highly heat tolerant material that can maintain the nozzle geometry for the duration of the burn. An aluminum nozzle retainer was designed to hold the graphite nozzle in place. To avoid losing engine efficiency both components were fitted with a double diametric O-ring seal. A compression ratio of 20.8% and 20.28% was acquired for the graphite nozzle and the aluminum retaining ring using **Equation 11**.

$$Compression\ Ratio = \frac{CS_{ORing} - GlandDepth}{CS_{ORing}} x100$$

Equation 11 – Compression Ratio

It should also be noted that the O-ring groove on the flanged section between the casing and the injection plate has a compression ratio of 28% since static face seals are generally required to have higher compression ratios for better functionality.[8] All O-ring measurements were also taken to have between 0-5% stretch as recommended using **Equation 12**.[8]

$$stretch = \frac{ID_{gland} - ID_{ORing}}{ID_{ORing}}$$

Equation 12 – Stretch

The aluminum casing's combustion chamber region (shown in blue in **Figure 7**), is an ablative material that was formulated and briefly tested by the rocket design team. The team's brief testing showed that a material of approximately 3/8" thickness can melt a penny on the surface of the material using a blow torch for a period of ~100 seconds before a thermocouple on the opposite side of the material shows temperatures over 100F. The ablative is a heat protection component that stops the aluminum casing from being over-heated during motor burn, and thus exploding. It is a pourable material that can be casted to shape. The rocket design team's student members will be creating a casting tube to provide the necessary component for the engine.

The injector plate is designed to provide a mixture ratio of 4:1 for the oxidizer and fuel, respectively. The geometry of the plate was designed to encourage a good mixture of fuel and oxidizer in the combustion chamber such that there will be an efficient burn in the engine. A reference injection plate geometry and the resources to characterize the plates were provided by Charles Campbell.[1] As designed, the injector plate contains 6 ports total. One port will be used to get readings for a pressure transducer, a single port with 4-1mm diameter injection lines will be used for the fuel, and 4 ports each containing a single 1.89mm diameter port will be used for the oxidizer. These diametric values were acquired from Heisters Rocket Propulsion book, using the discharge coefficient (C_D) based equation to solve for mass flow, as seen below in **Equation 13**.

$$\dot{m}_e = C_D A \sqrt{2\rho g \Delta p}$$

Equation 13 – Mass Flow with Discharge Coefficient

However, since the mass flow rate is known from the Rocket Propulsion Analysis program, one can back-solve for injection area for fuel and oxidizer separately. This equation also requires pressure drop across the injection plate. Heister states that it is of the utmost importance that the pressure drop be between 5-50% of the combustion chamber pressure (which is 400psi), thus the team designed the engine to have an 80 psi pressure drop which is 20% of the combustion chamber theoretical pressure.[6] ¼" NPT to ¼" AN pipe fittings were used to attach the feed systems to the injector plate. AN fittings are typically used in high pressure, rigid piped feed systems since they are designed to be fitted with a flared tube face which is compressed onto the 37-degree angle face of the fitting. ¼" NPT tapered fittings are used on the injector plate side for their good face mounting capabilities and diametric size, which is needed for the injector plate design.

To update the design considerations, a pressure transducer port was included into the model using the same ¼" NPT to ¼" AN on the injector plate. The pressure transducer, which was donated by The Spaceship Company, a Stellar Technologies AN port 0-5000psi range transducer, will not be able to handle the 3000K theoretical combustion chamber temperature that is expected. Thus, the pressure transducer will actually be installed on a line leading off of the tank that will have thermal insulation paste. Pressure will still be able to read through the thermal insulation paste, although a small data damping coefficient and error may likely be present when recording pressure.

Figure 7 – Cross Section View of the Motor

2.2.2. FEED SYSTEM

The piping and instrumentation diagram, shown below in **Figure 8**, utilizes many complex systems brought together to accomplish the most cost-effective, yet safe approach to creating a feed system that includes controls, data acquisition, and safety relief devices.

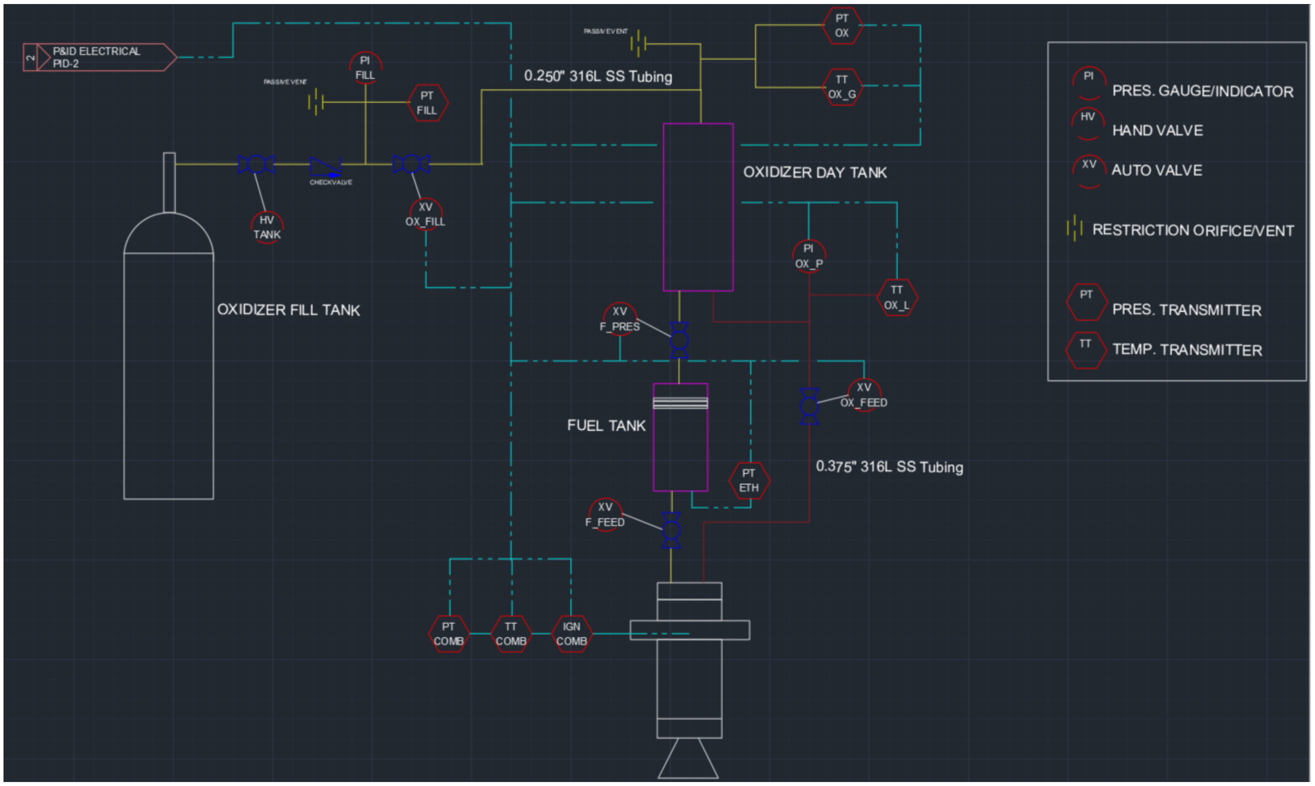

Figure 8 – Piping and Instrumentation Diagram of Current System

2.2.2.1. TUBING AND FITTINGS

Piping and fittings are extremely important in characterizing the extent at which an engine may be able to perform. The engine design itself has feed rate requirements that must be satisfied based on how much material can flow to the injector plate at any given time. The injector plate requirements are set to the values mentioned in **Table 1**.

Input Rocket Propulsion Analysis Data	
Oxidizer Mass Flow	**kg/s**
	0.083837
Fuel Mass Flow	**kg/s**
	0.20959
Chamber Pressure	**psi**
	400

Table 1 – Input Rocket Propulsion Analysis Data

The piping dimensional requirements will need to be different with regards to the fuel and oxidizer. The oxidizer mass flow rate, being higher, requires a larger pipe dimension. Therefore, 3/8" 316L Stainless Steel tubing was selected for the oxidizer. 316L Stainless Steel is a fantastic material when affordable. It has excellent chemical resistivity and has a high-pressure rating for smaller tubing, which is widely known. The current tubing, donated by the University of Akron, is Swagelok High Purity Stainless Steel Tubing, with a pressure rating of 3,330psi. This yields an effective factor of safety of 3+ for the working pressure of the oxidizer portion of the system. 1/4" 316L Stainless Steel is used on the fill line and fuel lines, since flow rate is less of a concern upon filling the oxidizer day tank and the mass flow rate requirement for the fuel is lower.

Using a simple mass flow rate equation in regard to material density and area of the pipe, the velocities of the liquids within each piping size is calculated and can be seen below in **Table 2**. The goal is to keep each pipe's speed underneath Mach 0.3, which is well known as the point where turbulent flow begins.

Piping Sizes and Flow Velocities			
Material			
316L SS	**Pipe Size**	**3/8"**	**Flow Area (in^2)**
	ID (Assuming 0.035" Wall Thickness)	0.305	0.07306166415
	OD	0.375	
	Pipe Size	**1/4"**	**Flow Area (in^2)**
	ID (Assuming 0.035" Wall Thickness)	0.18	0.02544690049
	OD	0.25	
	Oxidizer Flow Velocity	**(m/s)**	**Mach Value**
	1/4" Piping	64.92001235	0.18927113
	3/8" Piping	22.61121634	0.06592191353
	Fuel Flow Velocity	**(m/s)**	**Mach Value**
	1/4" Piping	16.18044126	0.04717329812
	3/8" Piping	5.635542023	0.01643015167

Table 2 – Piping Sizes and Flow Velocities

Fittings for the system will be Army-Navy (AN) style flared fittings. AN flared fittings are 37 degree angle fittings that are typically used in heavy-duty, off-roading, and aerospace applications, as they are stronger and more robust than the typical 45 degree angle hydraulic flared fitting typically used on commercial over-road vehicles. All connections directly to piping will be flared, while adapters will be utilized when connecting valves and solid objects, such as manifolds and the engine injector plate, which will utilize ¼" NPT connections.

2.2.2.2. CONTROLS

The test system accounts for the usage of two LabJack T7 Pro data acquisition units, in which one will be used to control the system through the I/O ports, and the other will be used as a DAQ. The LabJack T7 Pro that will be utilized for the control system of the test stand can be seen below in **Figure 9**.

Figure 9 – LabJack T7 Pro DAQ Board

The current system was designed by Jon Davis and Jon Spencer due to their electrical expertise. In the future, the Akronauts avionics team will take over the design and verification of the controls system, as they have experienced computer and electrical engineering students on the sub-team. Preliminarily, electrically actuated valves will be placed on a system that uses high amperage rated relays, which will connect externally to an AC power source. This AC power source may be a generator or direct grid hookup. The LabJack T7 has digital I/O pins which will actuate the relays, sending power from the external power source to the valves to be actuated. This is shown in a simple diagram below in **Figure 10**.

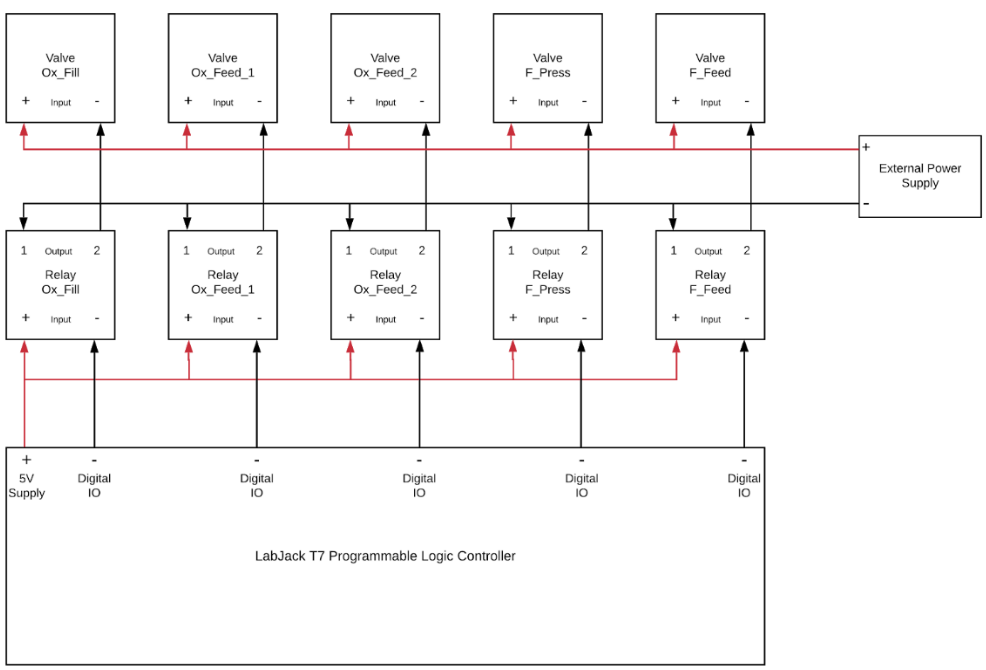

Figure 10 – Relay Wiring Diagram - Credits: Jonathan Davis

2.2.2.3. DATA ACQUISITION

All data acquisition devices are shown in **Figure 8**. Pressure transducers and thermocouples will be utilized at key points to understand and characterize the feed system while also recording and transmitting live data to make in-the-moment engine go or no-go decisions.

Thermocouples are chosen by type, with each type being differentiated by their rated values and precision. A breakdown of the thermocouple types can be seen below, in **Figure 11**. As each section of the system has differing temperature ranges, slightly different thermocouples will be utilized at different locations on the stand.

TOLERANCE OF THERMOCOUPLES						
	°C			°F		
ANSI/ASTM	Temperature Range	Standard	Special	Temperature Range	Standard	Special
T	-200° to -67°	± 1.5% T	± 0.8% T*	-328° to -88°	± 1.5% (T – 32)	± 0.8% (T – 32)*
	-67° to -62°	± 1°	± 0.8% T*	-88° to -80°	± 1.8°	± 0.8% (T – 32)*
	-62° to 125°	± 1°	± 0.5°	-80° to 257°	± 1.8°	± 0.9° *
	125° to 133°	± 1°	± 0.4% T	257° to 272°	± 1.8°	± 0.4% (T – 32)
	133° to 370°	± 0.75% T	± 0.4% T	272° to 700°	± 0.75% (T – 32)	± 0.4% (T – 32)
J	0° to 275°	± 2.2°	± 1.1°	32° to 527°	± 3.96°	± 1.98°
	275° to 293°	± 2.2°	± 0.4% T	527° to 560°	± 3.96°	± 0.4% (T – 32)
	293° to 760°	± 0.75% T	± 0.4% T	560° to 1400°	± 0.75% (T – 32)	± 0.4% (T – 32)
E	-200° to -170°	± 1% T	± 1°*	-328° to -274°	± 1% (T – 32)	± 1.8°*
	-170° to 250°	± 1.7°	± 1°*	-274° to 482°	± 3.06°	± 1.8°*
	250° to 340°	± 1.7°	± 0.4% T	482° to 644°	± 3.06°	± 0.4% (T – 32)
	340° to 870°	± 0.5% T	± 0.4% T	644° to 1600°	± 0.5% (T – 32)	± 0.4% (T – 32)
K	-200° to -110°	± 2% T	—	-328° to -166°	± 2% (T – 32)	—
	-100° to 0°	± 2.2°	—	-166° to 32°	± 3.96°	—
	0° to 275°	± 2.2°	± 1.1°	32° to 527°	± 3.96°	± 1.98°
	275° to 293°	± 2.2°	± 0.4% T	527° to 560°	± 3.96°	± 0.4% (T – 32)
	293° to 1260°	± 0.75% T	± 0.4% T	560° to 2300°	± 0.75% (T – 32)	± 0.4% (T – 32)
N	0° to 275°	± 2.2°	± 1.1°	32° to 527°	± 3.96°	± 1.98°
	275° to 293°	± 2.2°	± 0.4% T	527° to 560°	± 3.96°	± 0.4% (T – 32)
	293° to 1250°	± 0.75% T	± 0.4% T	560° to 2300°	± 0.75% (T – 32)	± 0.4% (T – 32)
R or S	0° to 1260°	± 1.5°	± 0.6°	32° to 1112°	± 2.7°	± 1.08°
	1260° to 1480°	± 0.25% T	± 0.1% T	1112° to 2700°	± 0.25% (T – 32)	± 0.1% (T – 32)
B	870° to 1700°	± 0.5% T	± 0.25%	1600° to 3100°	± 0.5% (T – 32)	± 0.25% (T – 32)
C**	0° to 426°	± 4.4°	—	32° to 800°	± 8°	—
	426° to 2315°	± 1% T	—	800° to 4200°	± 1% (T – 32)	—

Figure 11 – Thermocouple Chart by Thermometrics Corporation

A Type T thermocouple with a range from -325F to 700F is utilized on the oxidizer day tank to account for the possible near cryogenic temperatures and critical temperatures at over 100F. A Type J (32F to 1200F) thermocouple will be utilized for the feed system, to account for low temperatures and upper range temperatures that could be seen if back pressure events are noted in the feed lines, where combustion temperatures could be seen.

Pressure Transducers are also a vital component in determining if go/no-go conditions are present. It is equally as important as temperature in regards to the characterization of the feed system for the engine, as well as the pressure production in the combustion chamber. All these components will help verify functionality, or the lack thereof, upon cold flow and hot fire testing. Pressure sensors are simpler to pick, as 0-1000psi will be the range in which the Akronauts' system will function at the most. The feed system pressure will not exceed 1000psi, and the combustion chamber nominal theoretical value is 400psi. Therefore, any pressure transducer in that range with the chemical resistivity capable of handling the fuel and oxidizer should be capable of data acquisition if the accuracy of the transducer is within acceptable limits to the team.

2.2.2.4. *SAFETY DEVICES*

The tanks, while designed to withstand a large factor of safety over the vapor pressure of Nitrous between 70F-100F, will also be outfitted with a restriction orifice, also called a passive vent. The passive vent is used to constantly vent the oxidizer, like what is seen on major launch vehicles today. This helps keep tanks from experiencing an over-pressurization event during system fill, engine standby, and engine run phases. The Akronauts will size the passive vent in the future to accommodate a balance between material loss and pressure drop over time. The current sizing of the vent is currently approximated to be a hole with a diameter of 1mm.

Two passive vents are currently located on the system. One is directly off the oxidizer tank, which will experience the largest amount of pressure and will be the most safety critical as it is a student designed pressure vessel. The other vent is located directly on the fill line. This vent is designed to vent the fill line, such that the line will be atmospheric whenever test personnel would have to approach or the system. This is on the system such that a reliance on the automatic fill valve to depressurize the system is not necessary. This also doubles to remove excess material from the fill tank. This is valuable in the case that the team would use a simple racing nitrous tank, which comes in quantities slightly larger than the tank, so the rest of the material in the fill tank can safely vent to atmosphere.

2.2.3. TEST STAND

The test stand has been designed on a trailer to make the system portable. The design team recently got approval to store the system on campus, however the system will still need to be transported to the testing area from the storage location. The test stand assembly, seen below in **Figure 12**, is comprised of a reinforced frame for the thrust load cell, a set of rails for test sleds, test sleds to accommodate different motor types, and frames for securing tanks for liquid rocket engine testing. The designs of these four components were made with a goal of modularity in mind, as the system should be able to accommodate both liquid and solid motors in a variety of physical sizes and thrust capacities. Specific piping pathing, electronics locations, and the valve panel location are in the process of being finalized based off available space, thermodynamic impacts to the fluids, and material cost optimizations. The test stand will also use solenoid valves and an external power source to activate the solenoid valves. The team plans to use an external generator to achieve the needed power output for valve actuation. Data acquisition and controls of these mechanisms are also mentioned above in **FEED SYSTEM**.

Figure 12 – Current Test Stand Model

Although the liquid motor being designed in tandem with the test stand only produces a thrust of approximately 500 lbf, the reinforced frame for the thrust load cell was designed to be able to withstand tests of up to 2000 lbf without failing. The frame, seen below in **Figure 13**, will be secured to the trailer by bolts that pass through structural beams in the trailer, further increasing the rigidity of the system. ANSYS analysis indicates that the system can withstand thrust of over 3000 lbf without failing, giving the system a factor of safety of at least 1.5 when testing at maximum capacity, however further physical testing will be done to ensure the safety and strength of the system. The mounting point for the load cell can accommodate load cells ranging from 500 lbf capacity to 2000 lbf capacity, enabling the team to interchange load cells based on future testing needs. The reinforced frame assembly will be made from welded steel tube and can be seen in the figure below.

Figure 13 – Reinforced Frame Assembly

Rails were added to the test stand in order to accommodate a test sled for the system. This feature, as seen in **Figure 14** below, will aid the test stand functionality in several ways. The rails will support the weight of the motors and sleds being tested to prevent any moment forces from being applied to the load cells, it will ensure that the motor will be aligned properly with the load cell for testing, and it enables different motor sizes and types to be tested without changes to the test stand through the implementation of test sleds. This system was designed using extruded aluminum T-slotted rail due to the low cost of the material and compatible rail guides, the ease of assembly, and the availability of compatible brackets and hardware. Some linear support-rail shafts were donated to the Akronauts, however the cost of compatible rail guides for these rails exceeded the cost of acquiring new T-slotted rail, compatible guides for the T-slotted rail, and mounting brackets for the new rail.

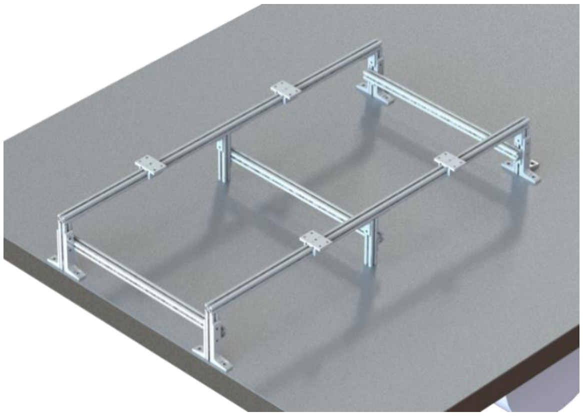

Figure 14 – Sled Guide Rails

The frame for securing liquid motor testing tanks was designed to accommodate a range of tank sizes for future testing. To account for the difference in size between the oxidizer and fuel tanks, the system will utilize two moveable base supports that will enable the team to align the top of the tanks. An adjustable collar that can be moved up or down on the frame will secure the top of the tanks. The combination of these two components will enable the system to accommodate a variety of tank sizes in the future. Spacing above and below the tanks will enable piping to be attached to the tanks, as well as facilitating the ability to refuel the tanks while mounted to the test stand. This system was designed using extruded aluminum T-slotted rail for its low cost and the wide availability of mounting brackets and hardware. Currently there are two frames for the fuel tanks on the stand; one set for the current testing tank designs that sit right behind the blast plate to minimize piping length to each other and to the motor, and one frame to support the larger fill tanks for the system. Both frames, seen below in **Figure 15**, are mechanically fastened to the test stand to make them easy to remove and reposition.

Figure 15 – Fuel Tank Support Frames

Structurally, the implementation of a test sled will ensure that the load cell solely bears the motors thrust as the sled and rails will support the weight of the motor and any other hardware or piping required to secure and operate the motor. Sleds will also enable new motors to be mounted to the system without having to adjust any structural components on the test stand itself. The current test sled can accommodate different liquid rocket engine designs by using a standardized mounting plate for the system. The 1:4 oxidizer distribution manifold for the current motor design is housed in a space between the motor and the blast plate, with mechanical attachments holding the system in place such that any future manifold designs can be easily implemented if needed. This space also leaves room for the piping to be installed between the motor and blast plate, allowing the team to utilize different piping layouts as needed with different future motors. For future solid rocket motors, either a different test sled could be designed to support the motor without a need for piping accommodations, or the motor being tested will need to incorporate a custom forward closure to attach the motor to the standardized mounting plate. To ensure the safety of the system, the strength of the test sleds will be verified using Finite Element Analysis (FEA). FEA of the current test sled can be seen in **DESIGN ANALYSIS**.

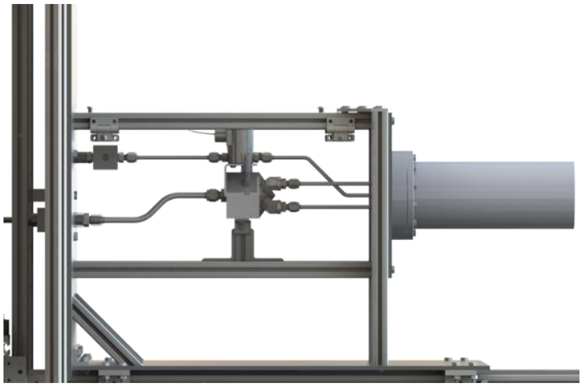

Figure 16 – Test Sled and System Piping

Although the type of piping being used in the system has been determined, the specific pathing of the piping is constantly changing as components and their locations are updated. The current design utilizes a combination of rigid and flexible piping. The current layout of the test sled piping can be seen above in **Figure 16**.

2.2.4. FUEL AND OXIDIZER TANKS

The liquid engine test stand houses two tanks to feed liquid nitrous oxide (oxidizer) and ethanol (fuel) to the injector plate of the liquid engine. The design of these tanks is important to ensure that they can hold the proper amounts of liquids and can withstand the pressure from these propellants. Both the oxidizer and fuel tanks have a similar external design, with slightly different input and output ports on their caps. The fuel tank also has a piston on the inside.

During the design phase for these tanks, two competing designs were considered by the team. These two designs were referred to as the flanged and un-flanged tank designs. The un-flanged design, see **Figure 17**, consists of two caps that fit into the tube with o-rings and retention rings. The flanged design, see **Figure 18**, consists of flanges welded to each side of the tank. The caps for the flanged tank bolt onto the flanges that are welded onto the tank. Each cap for both designs would have the necessary ports to ensure their respective liquid would be inputted and outputted properly.

Figure 17 – Un-Flanged Tank Design with Caps and Fuel Tank Piston

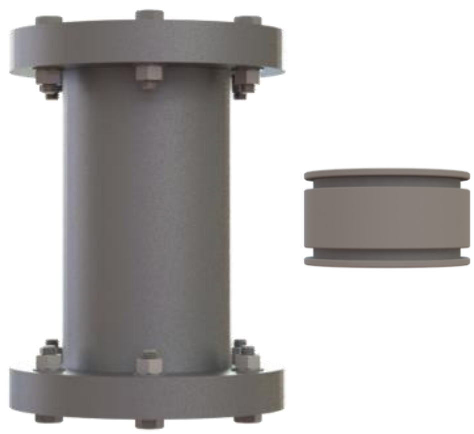

Figure 18 – Flanged Tank Design Assembly (Left) with Fuel Tank Piston (Right)

In order to determine which design was best for this application, the team made a decision matrix, see **Table 3**. The team considered the ease of design, ease of manufacture, reusability, safety, cost, and test stand integration. The tank's safety was determined to be the most important criterion since this system needs to be able to withstand pressure. Next, the ease of manufacture was determined to be the second most important criteria. Ease of manufacture is important to the team since students need to be able to fabricate this system. Since the Akronauts are planning on using this system for years to come, a system that can be remanufactured easily in the future if needed should be considered. Next, the team considered reusability. Reusability is important so components can be used multiple times to reduce waste and the need to remanufacture the tanks for every test. Test stand integration was equally as important as reusability, since the goal is to have the tanks held in place on the test stand with easy access to all ports. Lastly, the team considered ease of design and cost.

Tank Design Decision Matrix					
		Tank Options			
Criteria	**Weight**	**Un-Flanged Tank**		**Flanged Tank**	
		Score	Total	Score	Total
Ease of Design	0.10	6	0.60	9	0.90
Ease of	0.20	7	1.40	9	1.80
Reusability	0.15	7	1.05	10	1.50
Safety	0.30	6	1.8	10	3.00
Cost	0.10	10	1.00	7	0.70
Test Stand	0.15	6	0.90	10	0.90
Total	**1**		**6.75**		**8.80**

Table 3 – Tank Design Decision Matrix

Based on the criteria that was considered, the team determined that the flanged tank design would be the best design. Out of the criteria considered, cost was the only consideration that the flanged tank design was not the best. However, taking the reusability of the design into consideration makes the cost over time more effective even though the upfront cost is greater. The simplicity of the flanged tank design allows for easy manufacturing and assembly. The design is also safer overall.

To ensure that the flanged tank would be able to work in this application, analysis and calculations were conducted. These results can be found in **DESIGN ANALYSIS**.

The fuel tank assembly can be seen in **Figure 19**. This tank has one 1/4" NPT port on the top cap for a 1/4" tube OD x 1/4" ANPT male fitting. This fitting will connect to a fitting on the top cap of the oxidizer tank to control pressurization of the fuel tank. Inside of the fuel tank there is a piston with o-rings to ensure the pressurized gas from the nitrous oxide tank does not mix with the ethanol. This piston was also designed to ensure that it will not turn and get jammed into the tank. The bottom cap has two 1/4" NPT ports for one 1/4" tube OD x 1/4" ANPT male fitting and for one pressure transducer. The top and bottom cap fittings can be seen in **Figure 20**. The length between the caps of this tank is 7.87".

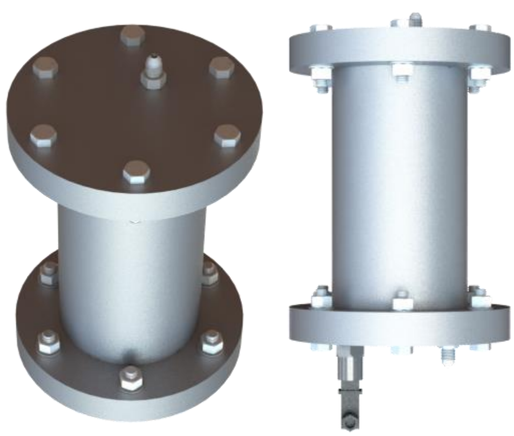

Figure 19 – Fuel Tank Isometric View (Left), Fuel Tank Side View (Right)

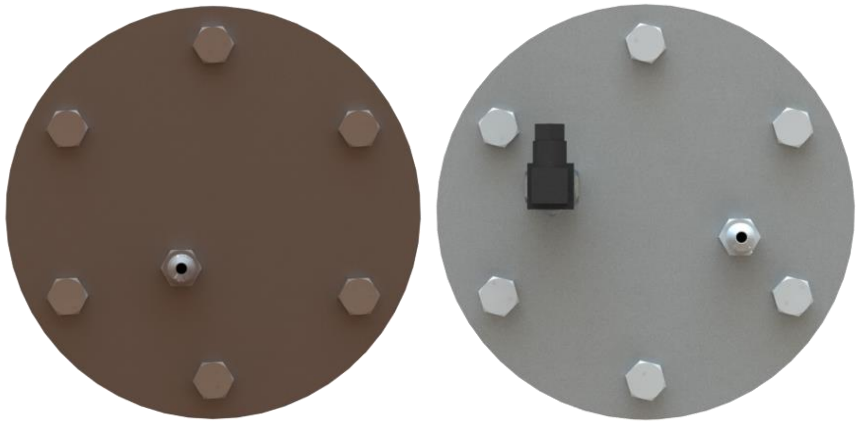

Figure 20 – Fuel Tank Top Cap (Left), Fuel Tank Bottom Cap (Right)

The oxidizer tank assembly can be seen in **Figure 21**. This tank has three 1/4” NPT ports on the top cap and one 1/8” vent hole. The three NPT ports are for a pressure transducer, a 1/4” tube OD x 1/4” ANPT male fitting, and a 3/8” tube OD x 1/4” ANPT male fitting. The 1/4” tube OD x 1/4” ANPT male fitting connects to the fuel tank cap fitting, as described in the previous paragraph. The bottom cap has two 1/4” NPT ports for one 3/8” tube OD x 1/4” ANPT male fitting and one thermal couple. The top and bottom cap fittings can be seen in **Figure 22**. The length between the caps of this tank is 22”.

Figure 21 – Nitrous Oxide Tank Isometric View (Left), Nitrous Oxide Tank Side View (Right)

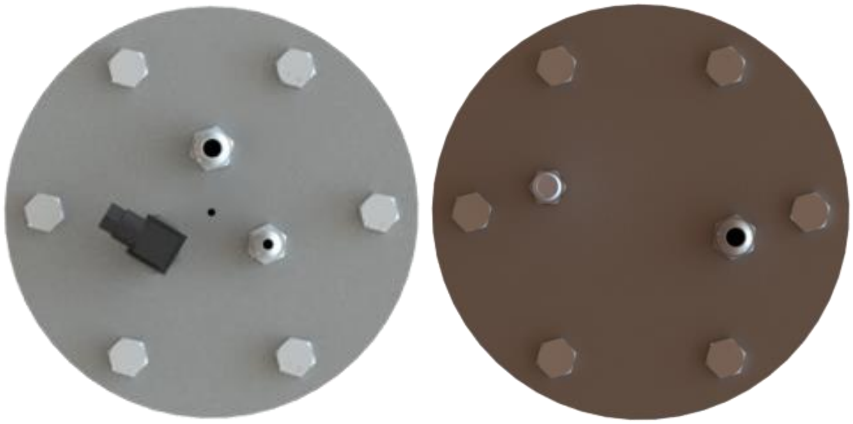

Figure 22 – Nitrous Oxide Tank Top Cap (Left), Nitrous Oxide Tank Bottom Cap (Right)

Both the fuel and oxidizer tanks have an outer diameter of 4” and an inner diameter of 3.625”. The flanges for these tanks both have a diameter of 6.5”. The flanges on both tanks are held together by six 3/8” bolts. The flanges that are welded onto each tank have two o-ring grooves to ensure that these tanks do not leak. Initially the team planned to only have one o-ring groove per flange; however, as an extra safety measure, the team added a second to ensure leaking does not occur.

3. DESIGN VERIFICATION

Testing procedures and design analysis were outlined to verify the design of the liquid motor and test system. The team also met with the University of Akron's safety department to get approval for the system and will continue to meet with the safety department to ensure the project proceeds in a safe manner.

3.1. TESTING PROCEDURES

To ensure project safety, physical testing of the constructed system will be completed. The team will also do preliminary testing to verify the working functionality of safety critical components and systems prior to any overall system test, such as cold-flow and hot-fire testing of the engine. This preliminary testing will include the testing of individual mechanical and electrical components as well as assembled subsystems. These tests will incorporate written documentation of the procedure and results to verify their completion and to better facilitate university safety approval for cold-flow testing and hot-fire testing of the completed and constructed project.

3.2. DESIGN ANALYSIS

Using hand calculations and FEA, the team verified that the factors of safety of the components and systems were at acceptable levels. FEA done in ANSYS shows that the reinforced frame for the load cell will be able to withstand 3000 lbf of thrust without exceeding the 46,000-psi yield strength of the steel used in the assembly. **Figure 23** shows that all areas of the frame experience less than 36,0000 psi of stress, indicating that the thrust support will have a factor of safety exceeding 1.5 should the team test a 2000 lbf motor in the future.

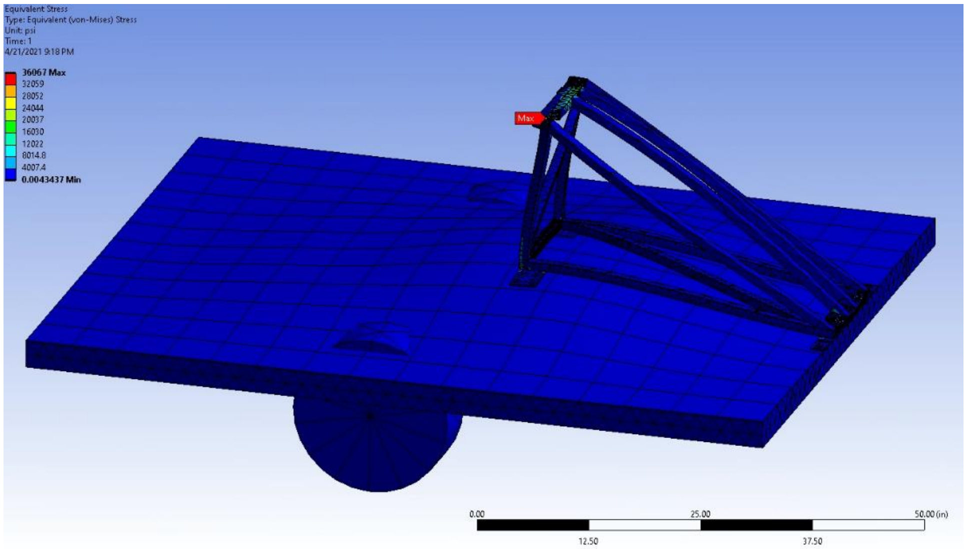

Figure 23 – Test Stand Stress Analysis

At 3000 lbf of thrust, the system will see a maximum deflection of 0.04 inches. The full results can be seen in **Figure 24.**

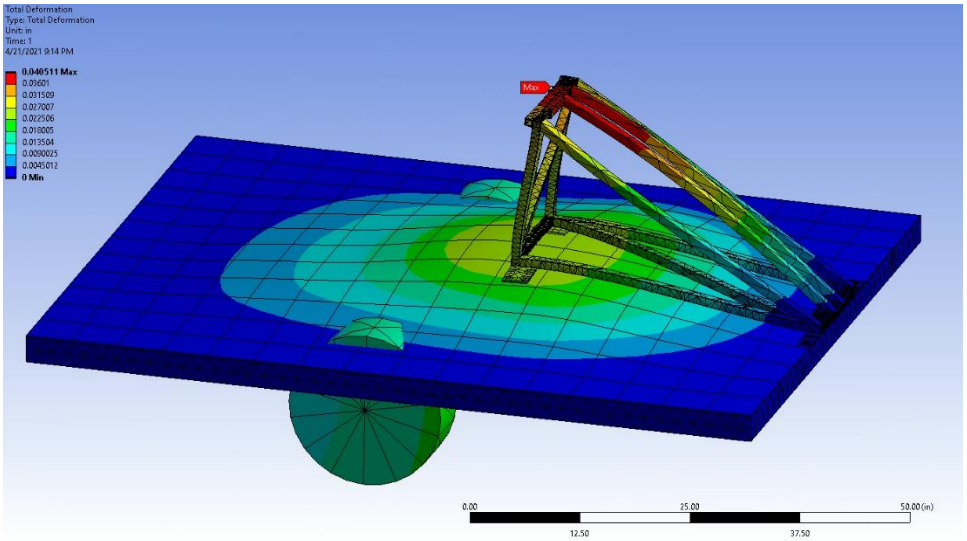

Figure 24 – Test Stand Deflection

The fuel and nitrous oxide tanks will have an operating pressure of approximately 750 psi. These tanks will be made of 6061 aluminum. Using the dimensions in **FUEL AND OXIDIZER TANKS**, the yield pressure for the tanks was calculated to be 3,442 psi. This gives the tanks a factor of safety of 4.59. The caps of the tanks will be secured with six 3/8" bolts. As the force at the ends of the tanks will be approximately 7,740 lbf and each bolt can withstand over 16,000 lbf of tensile loading, the caps will be secured by a factor of safety over 12.

FEA was conducted on the liquid rocket engine assembly in Abaqus by Dillon Petty. Focused analysis was also done on the injector plate, casing, and nozzle carrier for the liquid rocket engine to evaluate the loads experienced by these individual components. Load conditions for this analysis were set to 200% of the maximum expected load conditions. The analysis indicates that all components will be strong enough for their intended usage. Based on the stress values at the throat of the nozzle in the full assembly analysis, the graphite nozzle will have a factor of safety greater than 2. This analysis can be seen below in **Figure 25**.

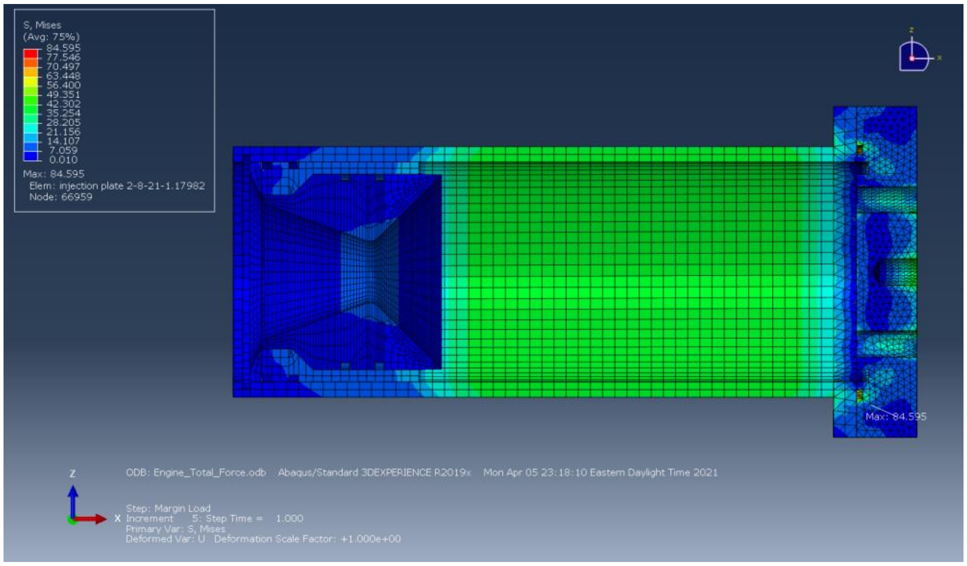

Figure 25 – Full Motor Assembly FEA Results

FEA on the injector plate shows a maximum stress of 84.6 MPa when put under 200% max loading conditions for thrust and internal pressure. At these extreme loading conditions, the 6061 aluminum component has a factor of safety of 3.25. The results of this analysis can be seen below in **Figure 26**.

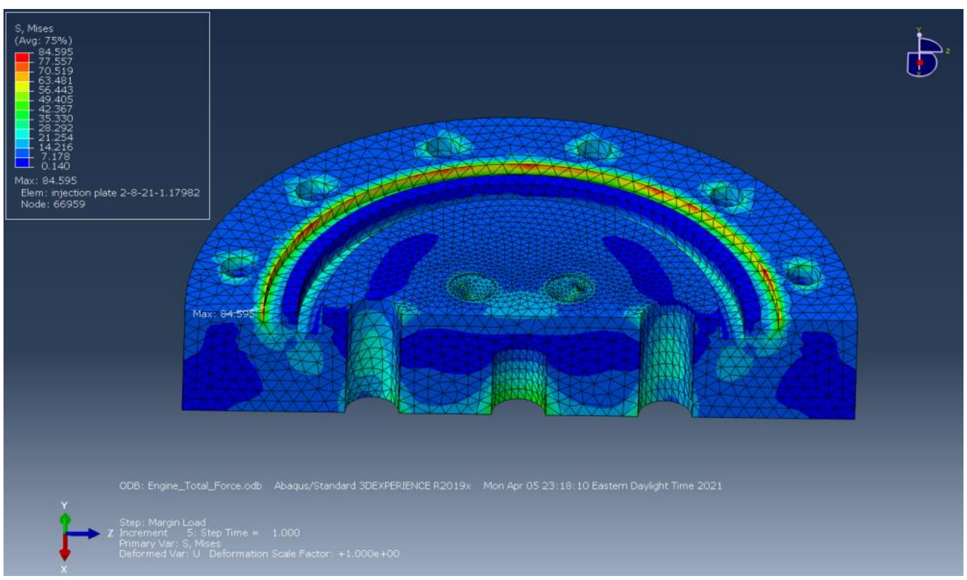

Figure 26 – Injector Plate FEA Results

FEA on the casing shows that the hoop stress at 200% loading conditions is 41 MPa. This result indicates that the 6061 aluminum casing will have a factor of safety of approximately 13 at max expected loading. The results of this analysis can be seen below in **Figure 27**.

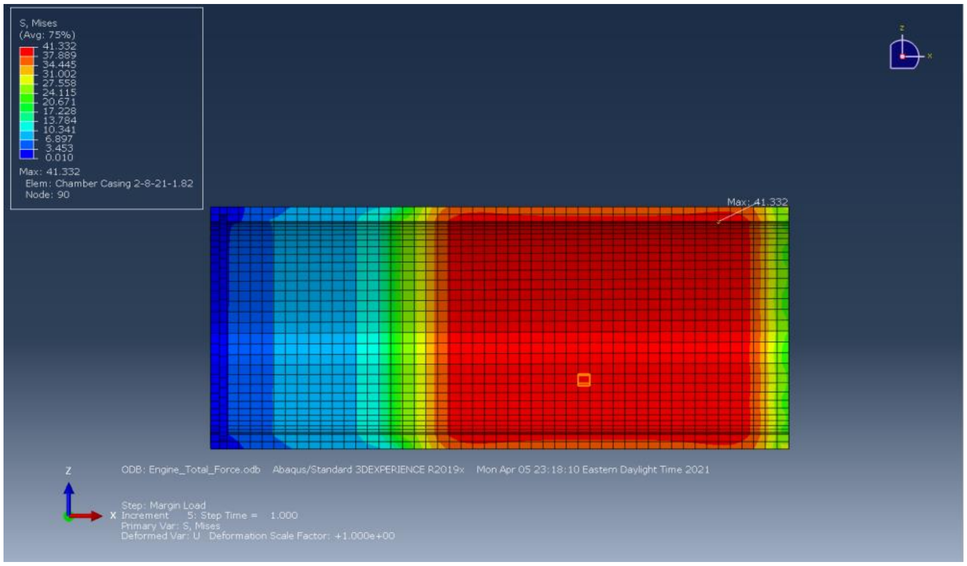

Figure 27 – Casing Hoop Stress FEA Results

FEA on the nozzle carrier shows a maximum stress of 19 MPa at 200% loading. At this extreme loading condition, the 6061 aluminum component will have a factor of safety of 14. The results of this analysis can be seen below in **Figure 28**.

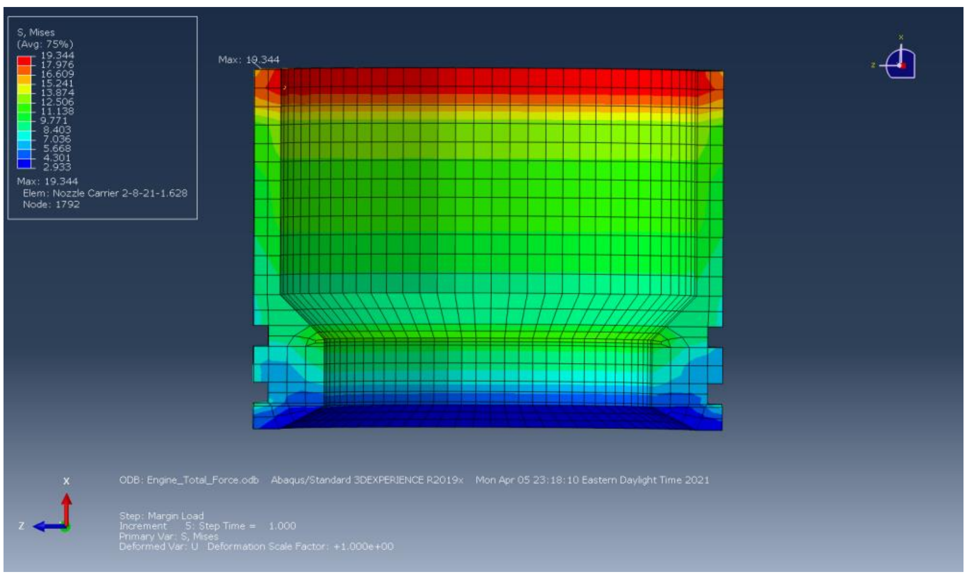

Figure 28 – Nozzle Carrier FEA Results

Initial FEA was also done on the preliminary test sled design to ensure that key components could adequately transfer the thrust load to the load cell and thrust support. This analysis was completed in Abaqus by Ryan Dippolito. Analysis of the blast shield under 200% expected load shows that the component will experience a max stress of 4,748 psi. Based on the components 40,000 psi yield strength, this component will have a factor of safety greater than 15 in expected loading conditions. The results of this analysis can be seen below in **Figure 29**.

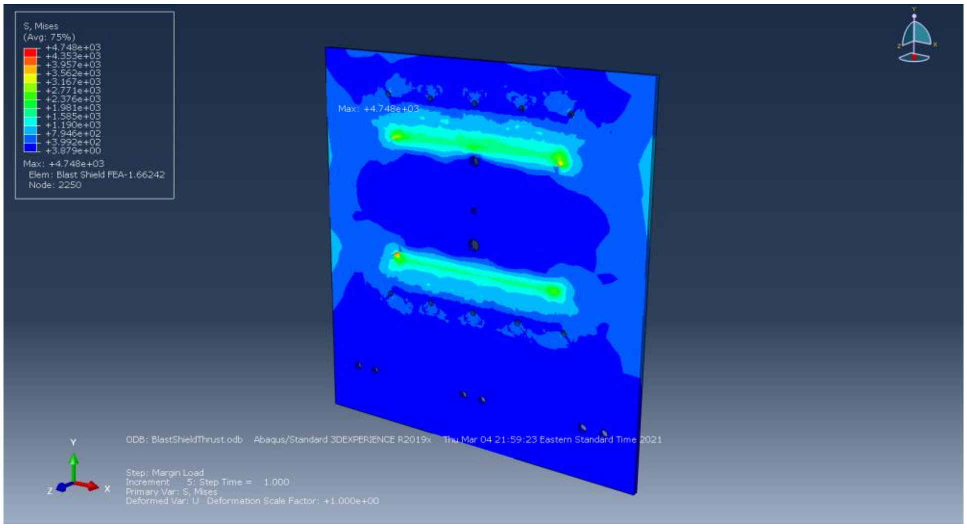

Figure 29 – Blast Shield FEA Results

FEA was also done on the engine mounting plate. Analysis shows that this component will experience a maximum stress of 27,440 psi at a 200% load. From the components 40,000 psi yield strength, this represents a factor of safety of 1.45 at 200% loading and a factor of safety of approximately 3 at maximum expected loading. The results of this analysis can be seen below in **Figure 30**.

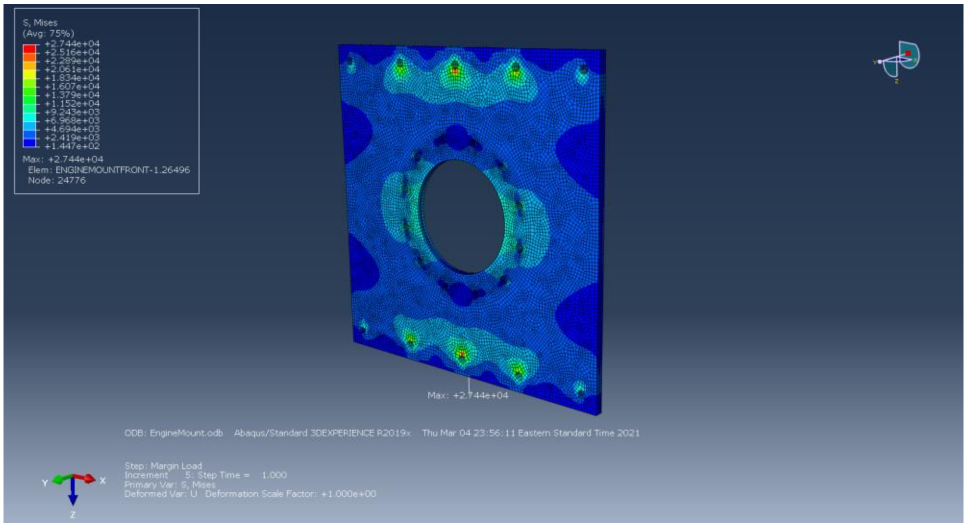

Figure 30 – Engine Mounting Plate FEA Results

As the piping and manifold components are updated and redesigned, FEA is continuously being done on them to ensure that they will be strong enough to ensure safe operation of the test stand. As the piping connecting the motor to the manifold and blast shield are rigid, this analysis combines both pressure and thrust loading conditions to ensure that any deflection in these components from the motors thrust will not cause any safety concerns for the system.

3.3. UNIVERSITY SAFETY APPROVAL

In early April, the Akronauts Rocket Design Team met with the University of Akron's safety department to discuss the possibility of moving forward with this project. During the meeting, the team discussed why it was important for the Akronauts to develop a liquid engine, the pros and cons of solid versus liquid propellants, types of propellant considered, pressure system options, the design so far, testing plans (cold flow and hot flow), safety considerations, and an updated schedule if the system was approved.

After the meeting, the Akronauts received safety approval to move forward with the fabrication of the test stand. The fabrication will take place in the University of Akron's Jet Propulsion building, see **Figure 31**, which will also serve as the current storage location for the test system. The team has not yet received approval to order chemicals or conduct testing; however, the safety department is going to help the Akronauts find a safe testing location and a safe way to obtain chemicals in the future.

Figure 31 – University of Akron's Jet Propulsion Building

3.4. RELEVANT DESIGN STANDARDS

In order to ensure the continued safety of the project, the team will continue to design and operate the liquid rocket engine and testing system in accordance with National Fire Protection Association (NFPA) code 1127. NFPA 1127: Code for High Power Rocketry "applies to the design, construction, limitation of propellant mass and power, and reliability of high power rocket motors and motor components, for use by a certified user for education, recreation, and sporting competition."[9] This standard is also the foundation for the high power rocketry safety codes of the National Association of Rocketry and Tripoli Rocketry Association, the two amateur high powered rocketry organizations that the Akronauts operate in under mentor guidance. [10,11]

4. COST AND SCHEDULE

A sub-section parts breakdown and schedule were created. All of these helped the team stay on track until the end of the Spring 2021 semester and helped keep the team organized with what still needs to be purchased, tested, and fabricated.

4.1. COST ANALYSIS

The current cost estimate for the liquid rocket engine and test system is **$8,387.36**. This estimate is comprised of the finalized components that the team needs for this project, and as such the cost of the project may change as new components are finalized or added to the system as necessary. This estimate does not include the cost of components that were donated to the team in the past, and currently includes the cost of components that may be donated to the team in the near future. A breakdown of this cost estimate by sub-section can be seen below in **Table 4**.

Total System Cost	
Sub-Section	**Cost**
Tanks	$732.09
Engine	$849.43
Valves	$1,503.94
Plumbing	$394.12
Electronics	$2,221.35
Test Stand	$1369.43
Ground Support Equipment	$692.59
Trailer	$0
Test Sled	$724.41
Total	**$8,387.36**

Table 4 – Total System Cost

4.2. SCHEDULE

The design, testing, and fabrication timeline is shown below in **Table 5**. The senior design team met Thursday and Friday evenings to discuss the progress of the project. During the Friday meetings, members of the Akronauts were involved to help ensure that the senior design team met the design team's needs. Unfortunately, COVID-19 and late semester safety approval altered the team's initial timeline, so the team had to make continuous modifications to the schedule. The team is still working with the Akronauts to make sure the finalized design can be fabricated and tested. The incomplete timeline tasks have been communicated with the Akronauts to facilitate a smooth transition between the senior design team and the Akronauts.

Project Timeline		
Target Completion Date	**Task**	**Status**
10/9/2020	Proposal Due Date	Complete
10/23/2020	Preliminary Research	Complete
10/30/2020	Progress 1 Report Due Date	Complete
12/10/2020	Preliminary Components Selected	Complete
12/11/2020	Progress Report 2 Due Date	Complete
1/1/2021	Preliminary Design 3D Models Created	Complete
2/1/2021	Preliminary Design Simulation Testing	Complete
2/15/2021	Critical Design	Complete
2/15/2021	Progress Report 3 Due Date	Complete
3/15/2021	Progress Report 4 Due Date	Complete
3/29/2021	Safety Approval Received from University	Complete
4/1/2021	Engine and Tank Design Finalized	Complete
4/18/2021	Design Day Presentation and Video Due	Complete
4/19/2021	Design Day	Complete
5/03/2021	Final Report Due	Complete
May	Finalize Test Stand Design	On-Going
May	Order Hardware and Components	On-Going
May	Test Components as They Arrive	On-Going
May	Build Sub-Systems and Assemblies as Components are Verified	On-Going
June	Finalize Safety Checklists and Procedures	On-Going
June	Engine, Test Stand, and Tank Fabrication Complete	Incomplete
June	Integrated Cold Flow Testing	Incomplete
July/August	Nozzle-Less Hot Fire Testing	Incomplete
August	Full Hot Fire Testing	Incomplete

Table 5 – Project Timeline

5. CONCLUSION

The team has considered their accomplishments, uncertainties, ethical considerations, and future work. All of these were outlined below.

5.1. ACCOMPLISHMENTS

The senior design team has finished the engine and tank designs, while the test stand, piping, and electronics system designs are near completion. Analysis through FEA and hand calculations for the engine and tanks were completed, determining that they should be safe for use in the final system. FEA for the test stand and test sled is still on going, as minor design changes are still being made. Comprehensive bill of materials have been made and ordered for a majority of the different components and sub-assemblies. Some key components are currently in the process of being finalized and incorporated into the models, and as such have not been ordered. The expected dimensions and capabilities of the test stand and liquid rocket motor have been discussed and approved by the Akronauts Rocket Design Team. The design team has also received University Safety Department approval to build and store the test stand, with approval for engine testing and propellant acquisition under review.

5.2. UNCERTAINTIES

This past year the university has added additional steps to the purchasing process for all student organizations regarding purchases over $200. Due to this change and the high cost of necessary components, it is uncertain how quickly the team will be able to acquire components for assembly and verification testing. It is also uncertain if or when these purchase restrictions will be lifted. After meeting with the university's safety department, the team has received university approval to build and store the test stand and liquid rocket engine on campus, however it is uncertain if or when the team will get approval to test the liquid rocket engine and where the team will be able to facilitate the testing.

5.3. ETHICAL CONSIDERATIONS

As this system uses hazardous chemicals, provides high pressure storage, combusts an oxidizer in a controlled manner, and electrically actuates high amperage valves, heavy considerations must be taken into the design of these items and into providing accurate calculations and proper factors of safety to all load and pressure bearing aspects to the system. Electrical design will also be considered for ethical considerations as the amount of DC current being transported to the controls system is more than enough to cause severe harm or even death to anyone working with it. Procedures and checklists will also be integral when determining safety of the system, and will be provided for safe handling of materials, hot fire tests, and cold flow tests.

5.4. FUTURE WORK

The foundation of this project, laid out by this senior design team, will help the Akronauts implement this liquid engine into a future rocket for competition. The senior design team will hand off this project to the Akronauts Rocket Design Team for fabrication completion, testing, and integration. Once fabricated, the test stand, fuel tank, and oxidizer tank can be tested to ensure that they are safe to use in their intended operation. Once the Akronauts and the University of Akron's safety department are confident in these components, the team will continue to cold flow testing. Once these tests have been successfully completed, the design team will proceed with combustion testing after gaining the University of Akron safety department's approval to do so.

6. ACKNOWLEDGEMENTS

Throughout this design process, the senior design team has collaborated with key members from the Akronauts Rocket Design Team in addition to our project's faculty advisors and project readers. At this time, special acknowledgements should be extended to:

Seth Arkwright
Jonathan Davis
Ryan Dippolito
Dillon Petty
Matthew Reppa (Alumni)
Lance Rosko
Dominic Salupo
Jonathon Spencer

These members and alumni have helped our senior design team with modeling, system analysis, and general engineering, as well as holding design reviews. These members are helping to make our senior project a system that is understood and usable for the design team after we graduate.

7. APPENDIX

7.1. APPENDIX A: EQUATION VARIABLES

Equation Variables	
Variable	**Description**
Q	Heat Flow Rate
k	Thermal Conductivity
L	Length of Cylinder
T_i	Internal Wall Temperature
T_e	External Wall Temperature
r_i	Internal Radius
r_e	External Radius
I_{sp}	Specific Impulse
F	Thrust
$\dot{m}$	Mass Flow Rate
g	Gravity
p_c	Chamber Pressure
p_t	Throat Pressure
γ	Specific Heat Ratio
A_t	Throat Area
a_t	Speed of Sound at the Throat
M_e	Mach at Exit
p_a	Atmospheric Pressure
A_e	Exit Area
V_e	Exhaust Velocity
p_e	Exit Pressure
ρ	Density
V	Velocity
A	Area
$\dot{m}_f$	Fuel Mass Flow Rate
$\dot{m}_{ox}$	Oxidizer Mass Flow Rate
r	Mixture Ratio ($\dot{m}_{ox}/\dot{m}_f$)
CS_{oring}	O-ring Cross Section Height
$GlandDepth$	Gland (Groove) Depth
ID_{gland}	Gland Inner Diameter
ID_{oring}	O-Ring Inner Diameter
C_D	Discharge Coefficient
Δp	Change in Pressure

Table 6 – Equation Variable Table

7.2. APPENDIX B: EQUATIONS FROM CAMPBELL ET AL[1]

Thrust is calculated by using the equation:

$$T = \dot{m}V_e + (p_e + p_o)A_e$$

Equation 14 – Thrust

Throat pressure is calculated by using the equation:

$$P_t = P_c\left[1 + \left(\frac{k-1}{2}\right)^{\frac{-k}{k-1}}\right]$$

Equation 15 – Throat Pressure

Throat area is calculated by using the equation:

$$A_t = \left(\frac{\dot{m}}{P_t}\right)\sqrt{\frac{R_U T_t}{MWk}}$$

Equation 16 – Throat Area

Exit Mach number is calculated by using the equation:

$$M_e = \sqrt{\left(\frac{2}{k-1}\right)\left[\left(\frac{P_c}{P_a}\right)^{\frac{k-1}{k}} - 1\right]}$$

Equation 17 – Exit Mach Number

The exit area is calculated by using the equation:

$$A_e = \left(\frac{A_t}{M_e}\right)\left[\frac{1 + \left(\frac{k-1}{2}\right)M_e^2}{\left(\frac{k+1}{2}\right)}\right]^{\frac{k+1}{2(k-1)}}$$

Equation 18 – Exit Area

The efficiency of this design is determined by using the equation:

$$\lambda = \frac{1 + \cos(\alpha)}{2}$$

Equation 19 – Design Efficiency

Characteristic length is determined by using the equation:

$$L^* = \frac{\zeta_2 * r_0^2 * \left(\frac{2}{k_c + 1}\right) * \left(\frac{k_c - 1}{2} * M_c^2\right)^{\frac{(k_c+1)}{2(k_c-1)}} * \sqrt{k_c * (MW_c) * T_{CO}}}{\frac{k_c}{C_{pc} * P_c} * \log(1 + B)}$$

Equation 20 – Characteristic Length

The Mach number in the chamber is determined by using the equation:

$$M_c = \frac{1}{C}$$

Equation 21 – Chamber Mach Number

Variable B is determined by using the equation:

$$B = \frac{C_{pc}(T_c - T_p)}{H_f}$$

Equation 22 – Variable B for Characteristic Length Equation

Variable S is determined by using the equation:

$$S = \frac{Pr_c}{2B}$$

Equation 23 – Variable S for ζ_2

Prandtl number of the gases in the chamber is determined by using the equation:

$$Pr_c = \frac{4k}{9k - 5}$$

Equation 24 – Prandtl Number for Chamber Gases

Stagnation temperature in the inlet is determined by using the equation:

$$T_{c0} = T_c\left(1 + \frac{k_c - 1}{2} * M_c^2\right)$$

Equation 25 – Inlet Stagnation Temperature

ζ_2 is determined by using the equation:

$$\zeta_2 = \frac{x_0 + 0.3}{2 + S}$$

Equation 26 – ζ_2 for Characteristic Length

The contraction ratio is determined by using the equation:

$$C = \frac{A_c}{A_t}$$

Equation 27 – Contraction Ratio

Chamber volume can be determined by working back through the equation:

$$L^* = \frac{V_c}{A_t}$$

Equation 28 – Used to Find Area of the Throat

The cross-sectional area for the injector ports can be determined by using the equation:

$$A = \frac{\dot{m}}{C_d\sqrt{2\rho(P_t - P_c)}}$$

Equation 29 – Injector Ports Cross-Sectional Area

The heat transfer coefficient can be determined by using the equation:

$$h_g = \left[\frac{0.026}{D_t^{0.2}}\left(\frac{\mu^{0.2}C_p}{Pr^{0.6}}\right)_{ns}\left(\frac{(p_c)_{ns}g}{c^*}\right)^{0.8}\left(\frac{Dt}{R}\right)^{0.1}\right] \times \left(\frac{A_t}{A}\right)^{0.9}\sigma$$

Equation 30 – Heat Transfer Coefficient

σ can be determined by using the equation:

$$\sigma = \frac{1}{\left[\frac{1}{2}\frac{T_{wg}}{(T_c)_{ns}}\left(1 + \frac{\gamma - 1}{2}M^2\right) + \frac{1}{2}\right]^{0.68}\left[1 + \frac{\gamma - 1}{2}M^2\right]^{0.12}}$$

Equation 31 – Solving for σ

Characteristic velocity can be determined by using the equation:

$$C^* = \frac{\sqrt{k_c R T_c}}{k_c\sqrt{\frac{2}{k_c + 1}^{\frac{k_c+1}{k_c-1}}}}$$

Equation 32 – Characteristic Velocity

The heat removed as the nitrous oxide vaporizes can be determined by using the equation:

$$\Delta Q = m_v H_v$$

Equation 33 – Heat Removed as Nitrous Oxide Vaporizes

The temperature change can be determined by using the equation:

$$\Delta T = \frac{-\Delta Q}{m_{liquid}C_{liquid}}$$

Equation 34 – Change in Temperature

Density can be determined by using the equation:

$$\Delta P = \frac{\dot{m}_{liquid}^2}{2\rho_{liquid}}\left(\frac{K}{\left(NA_{injector}\right)^2} - \frac{1}{A_{manifold}^2}\right)$$

Equation 35 – Density

Mass flow rate created by this change in pressure can be determined by using the equation:

$$\dot{m}_{liquid} = \sqrt{\frac{2\rho_{liquid}\Delta P}{D_{loss}}}$$

Equation 36 – Mass Flow Rate

The approximated loss factor that accounts for boundary effects can be determined by using the equation:

$$D_{loss} = \frac{K}{(NA_{injector})^2}$$

Equation 37 – Loss Factor

The true mass of liquid after a given time can be determined by using the equation:

$$m_{liquid} = \frac{\left(V_{tank} - \frac{m_{total}}{\rho_{vapor}}\right)}{\left(\frac{1}{\rho_{liquid}} - \frac{1}{p_{vapor}}\right)}$$

Equation 38 – True Mass of Liquid after a Given Time

8. REFERENCES

[1] Campbell, C., & Adkins, P. (2020). Design and Testing of a Low-Cost Bipropellant Liquid Rocket Engine (pp. 1-47, Rep.). Akron, OH: The University of Akron College of Engineering.

[2] Palacz, T. (2017). Nitrous Oxide Application for Low-Thrust and Low-Cost Liquid Rocket Engine. 7TH EUROPEAN CONFERENCE FOR AERONAUTICS AND SPACE SCIENCES (EUCASS).

[3] J.D. Lindbolm. Analysis of nitrous oxide as a propellant with selected fuels. Master's thesis, New Mexico Institute of Mining and Technology, 2013.

[4] Youngblood, S. H. (2015). Design and Testing of a Liquid Nitrous Oxide and Ethanol Fueled Rocket Engine. New Mexico Institute of Mining and Technology.

[5] N/A. (2015). Rocket Propulsion Analysis 2.3 Standard [Software]

[6] Edwig, R. (n.d.). Vapor Pressurization (VaPak) Systems History, Concepts, and Applications. Retrieved from http://www.holderaerospace.com/downloads/Technical_Papers/VaPak Systems Overview.pdf

[7] Heister, S., & Anderson, W. (2019). Rocket Propulsion. Cambridge University Press.

[8] No Name. (N.d.) O-ring Design Considerations. Marco Rubber. Retrieved from https://www.marcorubber.com/o-ring-groove-design-considerations.htm

[9] National Fire Protection Association. (2018). NFPA 1127: Code for High Power Rocketry. Retrieved from https://catalog.nfpa.org/NFPA-1127-Code-for-High-Power-Rocketry-P1410.aspx?icid=D729

[10] National Association of Rocketry. (2012). High Power Rocket Safety Code. Retrieved from https://www.nar.org/safety-information/high-power-rocket-safety-code/

[11] Tripoli Rocketry Association. (n.d.). Safety Code for High-Power Rocketry. Retrieved from http://www.tripoli.org/Portals/1/Documents/Safety%20Code/HighPowerSafetyCode%20-%202017.pdf